

Generation of Polythiophene Micropatterns by Scanning Electrochemical Microscopy

Caroline Marck,^{†,‡,§} Kai Borgwarth,^{†,‡} and Jürgen Heinze^{*,†,‡}

Freiburger Materialforschungszentrum (FMF), Stefan-Meier-Strasse 21, Albert-Ludwigs-Universität Freiburg, D-79104, Germany, and Institut für Physikalische Chemie, Albertstrasse 21, Albert-Ludwigs-Universität Freiburg, D-79104, Germany, and École Supérieure de Chimie, Physique, Électronique de Lyon (CPE Lyon), 43, Boulevard du 11 Novembre 1918, F-69616 Villeurbanne Cedex, France

Received April 12, 2000. Revised Manuscript Received November 30, 2000

The use of the scanning electrochemical microscope (SECM) is shown to be an effective tool for microdeposition of conducting polymers. A new concept of local polymerization applied to polythiophene is developed and discussed. The monomer dissolved in the solution is polymerized onto an oxidizing manganese dioxide surface, which is locally activated by tip-generated protons. An increase in resolution by a factor of 5 has been accomplished by the introduction of a chemical lens. The addition of a scavenger that reacts with the protons produced a significant focusing effect on the proton's diffusion field. Under these conditions, the resolution was achieved down to 8 μm with a 10- μm Pt electrode: the pattern was smaller than the tool used to generate it. We studied the effects of scavenger concentration, tip-surface distance, and scan rate on the structure's width. The patterns obtained were then successfully imaged by SECM and optical means.

1. Introduction

Scanning electrochemical microscopy (SECM) is a surface analysis and modification technique, which successfully combines features of scanning tunneling microscopy (STM) and ultramicroelectrodes (UMEs).^{1,2} A UME is moved in an electrolyte above the surface. The Faradaic current measured at the tip originates from oxidation or reduction of the electrochemical species in the solution and depends on both the chemical nature of the substrate and the tip-sample distance. The SECM has been shown to be a valuable analytical tool,³ and scanning the UME at a constant height provides valuable information about local surface conductivity, morphology, concentration profiles, and maps of reactive sites. Another field of application of this novel form of microscopy is surface modification. Micromodification, including deposition and etching processes, means well-defined, localized changes in chemical or physical properties.⁴ High-resolution surface etching and deposition have important technological implications for the fabrication of microelectronic devices.

On the other hand, conducting polymers such as polyaniline (PANI), polythiophene (PT), and polypyrrole (PPy) have attracted considerable attention in the microelectronics industry over the past decade. Because of their properties, their structural variability, and their great potential for commercial application, they have

rapidly become one of the most promising compounds in material science, e.g., for the fabrication of light emitting diodes, sensors, and optical waveguides.⁵ One of the most interesting aspects of these polymers is that they can be reversibly switched between electronically insulating and conductive states, accompanied by vast changes in their optical properties. This electronic conductivity and charge storage capacity have made conducting polymers very promising candidates as electrode materials in rechargeable polymer batteries.

This new generation of synthetic metals, with their fascinating variety of properties, such as enhanced stability and great structural variability, has a range of potential commercial applications, e.g., in Schottky diodes, field-effect transistors, photovoltaic devices, gas-separating membranes, artificial muscles or nerves, transparencies, antistatic coatings, conducting textiles, sensors, and biosensors.^{5,6}

(3) For example, see: (a) Kranz, C.; Wittstock, G.; Wohlschläger, H.; Schuhmann, W. *Electrochim. Acta* **1997**, *42*, 3105. (b) Bard, A. J.; Fan, F.-R. F. *Anal. Sci. Technol.* **1995**, *8*, 69A. (c) Wittstock, G.; Yu, K. J.; Halsall, H. B.; Ridgway, T. H.; Heineman, W. R. *Anal. Chem.* **1995**, *67*, 3578. (d) Horrocks, B. R.; Schmidtke, D.; Keller, A.; Bard, A. J. *Anal. Chem.* **1993**, *65*, 3605. (e) Borgwarth, K.; Ebling, D.; Heinze, J. *Electrochim. Acta* **1995**, *40*, 1455.

(4) (a) Hüsser, O. E.; Craston, D. H.; Bard, A. J. *J. Electrochem. Soc.* **1989**, *136*, 3222. (b) Mandler, D.; Bard, A. J. *J. Electrochem. Soc.* **1989**, *136*, 3143. (c) Mandler, D.; Bard, A. J. *J. Electrochem. Soc.* **1990**, *137*, 2468. (d) Zu, Y. B.; Xie, L.; Mao, B. W.; Tian, Z. *Electrochim. Acta* **1998**, *43*, 1683. (e) Hüsser, O. E.; Craston, D. H.; Bard, A. J. *J. Vac. Technol.* **1988**, *86*, 1873. (f) Mandler, D.; Bard, A. J. *J. Electrochem. Soc.* **1990**, *137*, 1079. (g) Meltzer, S.; Mandler, D. *J. Electrochem. Soc.* **1995**, *142*, L82. (h) Hess, C.; Borgwarth, K.; Ricken, C.; Ebling, D. G.; Heinze, J. *Electrochim. Acta* **1997**, *42*, 3065. (i) Mandler, D.; Meltzer, S.; Shohat, I. *Isr. J. Chem.* **1996**, *36*, 73. (j) Schultze, J. W.; Morgenstern, T.; Schattka, D.; Winkels, S. *Electrochim. Acta* **1999**, *44*, 1847. (k) Borgwarth, K.; Ricken, C.; Ebling, D. G.; Heinze, J. *Ber. Bunsenges. Phys. Chem.* **1995**, *99*, 1421.

(5) (a) Bäuerle, P. *Adv. Mat.* **1993**, *5*, 879. (b) Heinze, J. *Synth. Met.* **1991**, *41*, 2805.

* Author to whom correspondence should be sent.

[†] Freiburger Materialforschungszentrum.

[‡] Institut für Physikalische Chemie.

[§] École Supérieure de Chimie, Physique, Électronique de Lyon.

(1) Bard, A. J.; Fan, F.-R. F.; Kwak, J.; Lev, O. *Anal. Chem.* **1989**, *61*, 132.

(2) Engstrom, R. C.; Weber, M.; Wunder, D. J.; Burgess, R.; Winquist, S. *Anal. Chem.* **1986**, *58*, 844.

A fundamental challenge of these new materials is bringing them into structures of well-defined shapes. The SECM and its local polymerization possibilities have opened a new approach to microtechnological applications of conducting polymers, especially concerning sensors and electronic devices.

Some successful examples of the polymerization of conducting polymers using the SECM are described in the literature. Bard et al. first reported the microdeposition of polyaniline on platinum in the so-called direct mode.⁷ Later, Schuhmann et al. successfully deposited polypyrrole on gold-coated glass with a lateral resolution of 60 μm .⁸ In both works, the direct mode is shown to cause strong diffusion broadening, resulting in poor lateral resolution. Zhou and Wipf then reported the deposition of polyaniline patterns on gold, platinum, and carbon surfaces using pH shifts induced by the feedback mode of the SECM.⁹ Turyan and Mandler studied polyaniline on a SAM,¹⁰ and recently, our group was able to synthesize poly[2',5'-bis(1-methylpyrrol-2-yl)-thiophene] on PMMA with a lateral resolution as low as 15 μm .¹¹ This last method takes advantage of the insolubility of the monomer in aqueous solutions.

Here, we describe a new concept of microdeposition of conducting polymers using the SECM and an immobilized oxidant-coated sample. This new approach is suitable for monomers with high solubilities in water. As an application of this new method, the local polymerization of thiophene was performed on a manganese dioxide surface locally activated by tip-generated protons. Most radical cations and small oligomers are soluble in water, whereas uncharged octamers and larger molecules are not and deposit on the surface. The principle of using MnO_2 -covered surfaces to enable the deposition on conducting polymers and, thereby, to make the surface conducting is technically applied, e.g., to fill drill holes in printed circuit boards with subsequently galvanically deposited copper.¹²

2. Experimental Section

A home-built bipotentiostat was used to adjust the ultramicroelectrode (UME) potential with respect to a silver quasi reference electrode. A platinum wire served as a counter electrode. The UME was moved in all three dimensions by means of piezoelectric scanners (PX-400, Piezोजना, Jena, Germany) that enabled movements of up to 400 μm . An additional stage (MT 65, Micos, Umkirch, Germany) that was driven by a step motor was incorporated for large translations in the vertical direction. A personal computer and the associated A/D and D/A card (ML8-486, Sorcus, Germany) electronically controlled the electrochemical parameters and positions. An inverse optical microscope (Axiovert, ZEISS) mounted

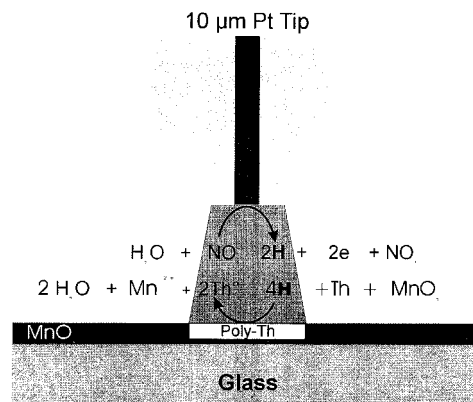


Figure 1. Schematic representation of the deposition of polythiophene using the SECM.

under the electrochemical cell has been shown to be a very powerful tool for controlling the microstructuring processes in situ, for the observation and prevention of abnormal phenomena such as gas bubble formation. The introduction of a camera (Olympus, DP 10) allowed us to take numerical pictures during polymerization.

Disk-shaped UMEs of 10 μm diameter were made by sealing platinum wire (Goodfellow, Cambridge) in a soft glass tube that was subsequently ground at one end. The glass sheaths were cylindrically shaped with an outer diameter of approximately 100 μm . Prior to use, the UMEs were polished using diamond pastes (3 and 0.25 μm , Winter & Sohn).

The electrolyte consisted of an aqueous solution of 20 mM thiophene (Aldrich), 40 mM potassium nitrite KNO_2 (Merck) to generate protons by oxidation, sodium bicarbonate NaHCO_3 (Merck) as a scavenger in concentrations up to 40 mM, and 10 mM potassium hexacyanoferrate(III) $\text{K}_3[\text{Fe}(\text{CN})_6]$ (Fluka AG) as a mediator. KCl (Merck) was used as a conducting salt when no scavenger was used. The samples used were manganese dioxide surfaces, which were obtained by sputtering on glass (sputter machine Edwards, Auto 306) in a 5×10^{-2} mbar argon atmosphere at 250 W for 45 min. The MnO_2 sputter target was fabricated by drying an aqueous emulsion of MnO_2 powder (Riedel-De Haen AG, Seelze-Hannover) in a Petri dish. The homogeneous brown surface of samples of some 100 nm thickness might be a mixture of nonstoichiometric manganese oxides MnO_{2-x} .

In a typical SECM experiment, a MnO_2 -covered glass substrate was mounted in a cell, and the UME was made to approach the substrate. The UME reduced hexacyanoferrate(III) under diffusion control. The UME was stopped once the steady-state current increased by ca. 10% over the value attained when it was far above the substrate.

3. Results and Discussion

The formation of polythiophene from its monomer proceeds via an oxidation process that is driven by a manganese dioxide surface in a local acidic environment. Figure 1 summarizes the principle of this synthesis. The principle of fabricating microstructures is based on the local generation of protons to make the electrolyte acidic in the vicinity of the tip. This locally controlled and irreversible generation of protons occurs by oxidizing nitrite ions in the solution.

(6) (a) Ratcliffe, N. M. *Anal. Chim. Acta* **1990**, *239*, 257. (b) White, H. S.; Kittleson, G. P.; Wrighton, M. S. *J. Am. Chem. Soc.* **1984**, *106*, 5375. (c) Yoneyama, H.; Wakamoto, K.; Tamura, H. *J. Electrochem. Soc.* **1984**, *106*, 5375. (d) Schuhmann, W.; Kranz, C.; Huber, J.; Wohlschlager, H. *Synth. Met.* **1993**, *61*, 31.

(7) Wu, Y.-M.; Fan, F.-R. F.; Bard, A. J. *J. Electrochem. Soc.* **1989**, *136*, 885.

(8) Kranz, C.; Ludwig, M.; Gaub, H. E.; Schuhmann, W. *Adv. Mat.* **1995**, *7*, 38.

(9) Zhou, J.; Wipf, D. O. *J. Electrochem. Soc.* **1997**, *144*, 1202.

(10) Turyan, I.; Mandler, D. *J. Am. Chem. Soc.* **1998**, *120*, 10733.

(11) Borgwarth, K.; Rohde, N.; Ricken, C.; Hallensleben, M. L.; Mandler, D.; Heinze, J. *Adv. Mat.* **1999**, *11*, 1221.

(12) Technique applied by Atotech GmbH, Berlin, Germany.

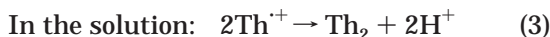


On the surface, the first step of the reaction of thiophene with manganese dioxide in an acidic environment produces soluble radical cations and Mn^{2+} ions.

On the surface:



Subsequently, pairs of radical cations couple to form dimers as follows:



The dimers are then oxidized to radical cations, which, after coupling to σ -oligomers, again undergo deprotonation to form tetramers. Subsequent multistep coupling leads to oligomers. The thiophene radical cations and small oligomers are soluble in water to some extent, whereas the octamers and larger molecules are not and deposit on the surface. Thus, the degree of polymerization of the oligomers synthesized in this way is probably larger than 8. Deposited polymer can undergo chain coupling in the solid state. However, the reactivity of the oligomers decreases with the degree of polymerization, because of the delocalization of the positive charge in the radical cations. This limits chain lengths to about 20–30 units.

As pointed out before, a critical parameter in the experiments is the pH. Figure 2 shows the Pourbaix diagram of all species involved and reveals that the polymerization window is quite narrow. As can be determined from the graph, the suitable range for manganese dioxide to oxidize thiophene lies below pH 3. The more acidic the environment, the larger the degree of polymerization will be. To provide such a pH under the tip, the nitrite concentration as a function of the diffusion coefficients is estimated to be higher than 2 mM. The thiophene concentration was taken as 20 mM, close to the limit of solubility, to enable fast modification based on the second-order polymerization reaction. $\text{K}_3[\text{Fe}(\text{CN})_6]$ was chosen as a second mediator for analytical purposes and KCl as a conducting salt when no scavenger was used. The Pourbaix diagram shows that the reduction of manganese dioxide by nitrite ions competes with the main reaction; hence, the nitrite concentration was kept below 50 mM.

It was found empirically that some electrochemical polymerization occurs at the UME. This leads to the covering of the electrode and might cause the current to drop continuously. As a result, the initial structures generated at constant potential were not uniform. To prevent such a drop, the microstructuring was performed in a galvanostatic process. This alternative has been shown to be efficient and to allow for a precise and reproducible control of the structure fabrication. Patterns were formed galvanostatically by scanning the UME across the surface at 20 nA. At this current, nitrite ions were oxidized, and protons were generated under the tip.

Figure 3 shows a polythiophene structure, which was obtained by scanning a 10- μm Pt electrode for 200 μm . The polymer stripe can be clearly identified on top of the remaining MnO_2 . It is 205 μm long and about 75 μm wide. The lateral resolution is poor, and the edges

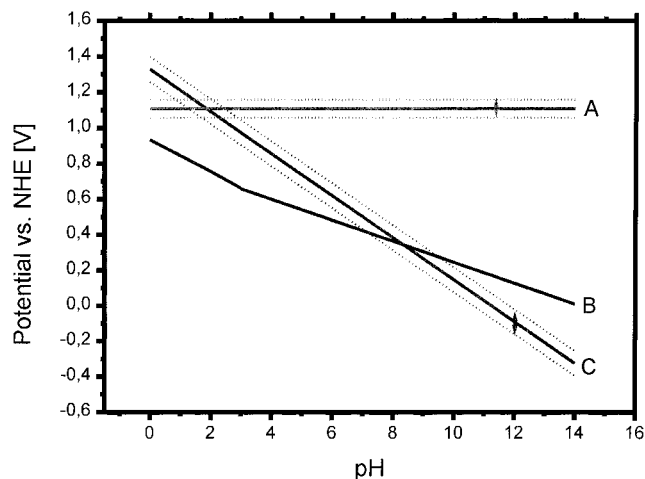


Figure 2. Pourbaix diagram of (A) thiophene, experimental value of polymerization potential and errors $E^p = +1.108 \text{ V} \pm 0.050 \text{ V}$; (B) nitrite, theoretical determination $E^p(\text{NO}_3^-/\text{NO}_2^-) = +0.934 \text{ V} - (0.0887 \text{ V}) \times \text{pH}$ if $\text{pH} < 7$, and $E^p(\text{NO}_3^-/\text{NO}_2^-) = +0.836 \text{ V} - (0.059 \text{ V}) \times \text{pH}$ if $\text{pH} > 7$; (C) manganese dioxide, $E^p(\text{MnO}_2/\text{Mn}^{2+}) = +1.224 \text{ V} - (0.118 \text{ V}) \times \text{pH} - (0.029 \text{ V}) \times \log[\text{Mn}^{2+}]$, experimental value and errors at $\text{pH} = 7$, $E^p(\text{MnO}_2/\text{Mn}^{2+}) = +0.502 \text{ V} \pm 0.070 \text{ V}$. Standard reduction potentials taken from Lide, D. R. *Handbook of Chemistry and Physics*, 77th ed.; CRC Press: Boca Raton, FL, 1996–1997; pp 8–21.

are blurred. This phenomenon is probably due to the lateral diffusion of the protons generated at the tip, which causes a halo around the structure. The introduction of a scavenger into the electrolyte to limit proton diffusion has been shown to be an excellent way of enhancing the resolution of the microstructuring.

The basic principle of the chemical lens was recently reported by K. Borgwarth and J. Heinze:¹³ the tip-generated species diffuse from the center to the outer vicinity, whereas the scavenger moves in the opposite direction. If the chemical reaction between the scavenger and the protons is fast enough, it will be spatially limited to a thin zone surrounding the tip where the two species meet. Within this zone, the tip-generated protons dominate, and the environment is acidic, whereas the amount of scavenger is negligible, and the opposite is true outside this zone. As the distance increases, so does the flux of scavenger, whereas the flux of protons in the vertical direction decreases. This results in a better lateral resolution with increasing distance. Figure 4 shows the principle of this concept schematically.

Several buffers were tested at various pHs, and most of them accentuated the phenomenon of adsorption on the UME. Only sodium bicarbonate at pH 7 gave acceptable results. At pH 7, the anion HCO_3^- dominates in the solution, whereas at pH 2–3, within the lens, the buffer is in its acidic form, H_2CO_3 . These considerations allow for the use of the sodium bicarbonate as a scavenger for the application of a chemical lens. To understand the patterning process and the chemical lens phenomenon, a set of experiments was conducted in which we systematically varied the scan speed and the tip–substrate distance. The thin lines result from scanning the UME at fixed scan speed while continuously increasing the tip–substrate distance at a fixed slope. This set of experiments was conducted with

(13) Borgwarth, K.; Heinze, J. *J. Electrochem. Soc.* **1999**, *146*, 3285.

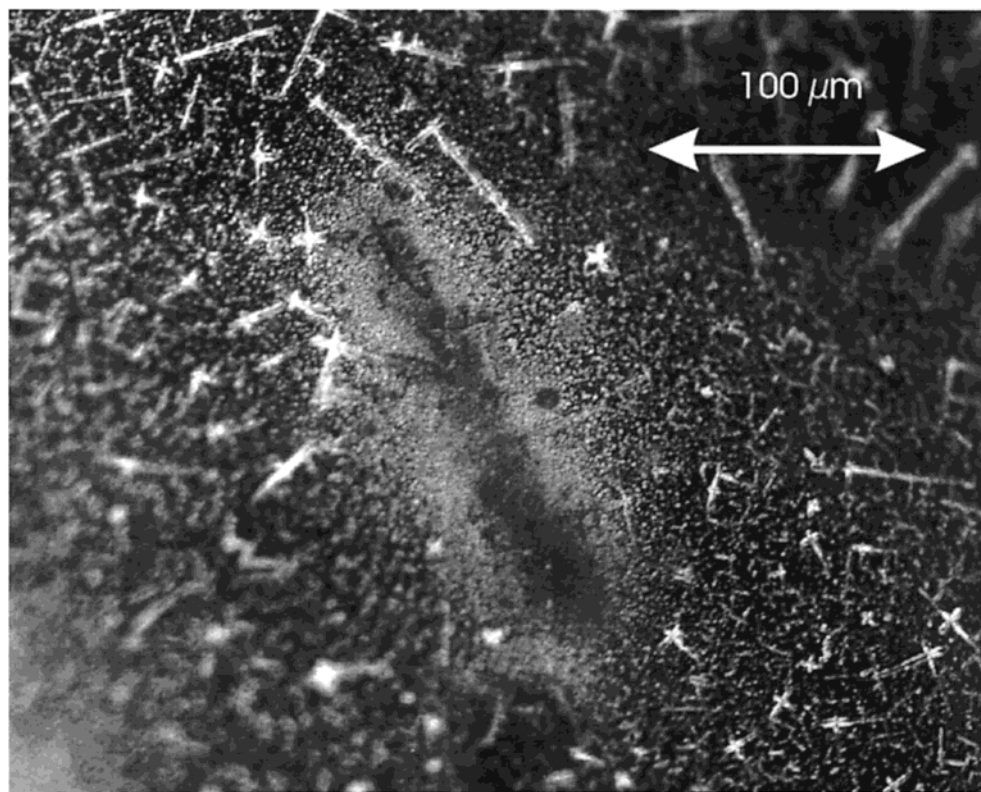


Figure 3. Microdeposition of polythiophene on MnO_2 surface. Tip = $10\text{-}\mu\text{m}$ Pt, RG = 10; electrolyte = 40 mM KNO_2 , 20 mM thiophene, 10 mM $\text{K}_3[\text{Fe}(\text{CN})_6]$, 1 M KCl. Scan rate = $1\ \mu\text{m/s}$, 25 nA, at a distance of $10\ \mu\text{m}$ from the surface.

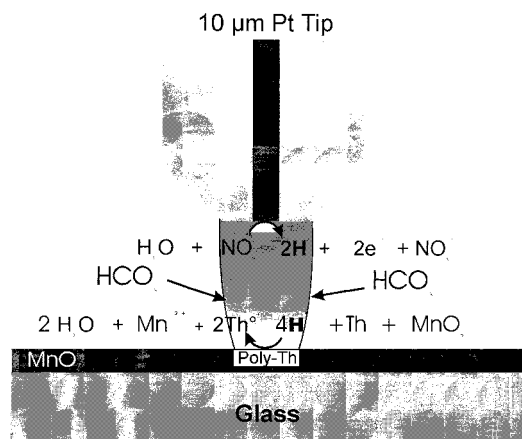


Figure 4. Schematic representation of the deposition of polythiophene using the SECM and the chemical lens.

several scavenger concentrations varying from 10 to 40 mM. The thiophene concentration was kept constant at 20 mM.

Figure 5 shows the result of such an experiment with a 30 mM concentration of sodium bicarbonate. Our initial observation was that the addition of a scavenger to the electrolyte had a significant focusing effect on the diffusion field. The structure width was reduced from 75 to $15\ \mu\text{m}$. Using suitable parameters, stripes of polythiophene were deposited that were found to be straight, smooth, and as small as the tip diameter. The structuring process was reproducible. Moreover, the optical microscope showed a very sharp delimitation of the edges of the structures. However, some of the lines presented irregularities in their triangular form. This problem was due to the current imposed by the galvanostatical process, which sometimes forced the

formation of oxygen bubbles from the aqueous electrolyte.

The five lines shown in Figure 5 illustrate the drastic influence of the scan speed and the tip–substrate distance on the structure width. Such dependence is depicted in Figure 6. With increasing scan speed and tip–substrate distance, the stripe's width fell continuously, even below the diameter of the tip, until deposition finally ceased. The experiment was repeated with just minor deviations from the previous deposition patterns. Bubble formation can be avoided by decreasing the current used for the microstructuring. We also established a linear dependence between the structure width and the tip–substrate distance.

The influence of scavenger concentration was also studied, and the experimental results are presented in Figure 7. As shown, the dimension of the structures decreases with increasing scavenger concentration. The oxidation of each nitrite ion generates two protons, and a 10 mM scavenger concentration represents 25% of the nitrite bulk concentration. When the scavenger concentration rises to 40 mM, i.e., to 100% of the nitrite concentration, most protons are caught, which explains why just a very narrow band of manganese dioxide is activated by the protons under these conditions. Comparing the slopes of the lines drawn in Figure 7 with those of other experiments using the chemical lens,^{13,14} it was found that significantly lower concentrations of scavenger (or more precise rationing of the scavenger and mediator concentrations) were sufficient to produce a similar focusing effect. The width and thickness of the generated pattern increase continuously during the

(14) Ufheil, J.; Boldt, F. M.; Börsch, M.; Borgwarth, K.; Heinze, J. *Bioelectrochemistry* **2000**, *52*, 103.

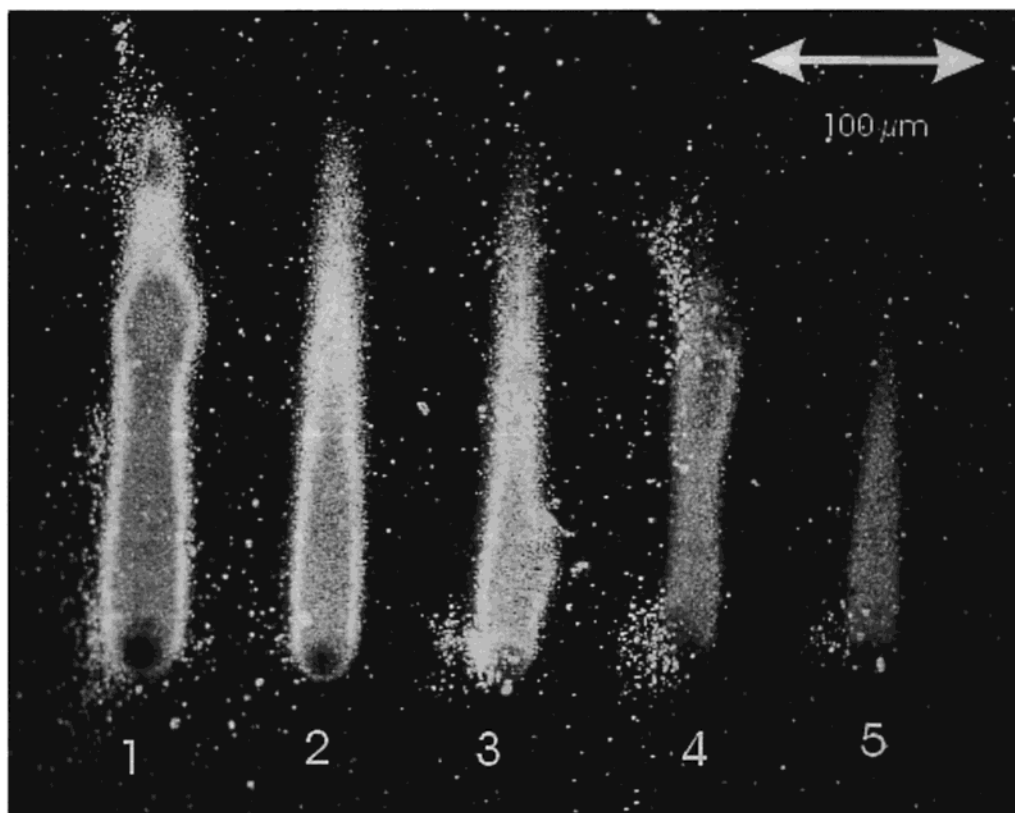


Figure 5. Tip = 10- μm Pt; RG = 5; electrolyte = 40 mM KNO_2 , 20 mM thiophene, 10 mM $\text{K}_3[\text{Fe}(\text{CN})_6]$, 30 mM NaHCO_3 . Galvanostatic process = 20 nA, beginning at a distance of 5 μm from surface, and then a slope of 0.07 until 26 μm from the surface. Scan rate = (1) 0.6, (2) 0.8, (3) 1, (4) 1.2, and (5) 1.4 $\mu\text{m}/\text{s}$.

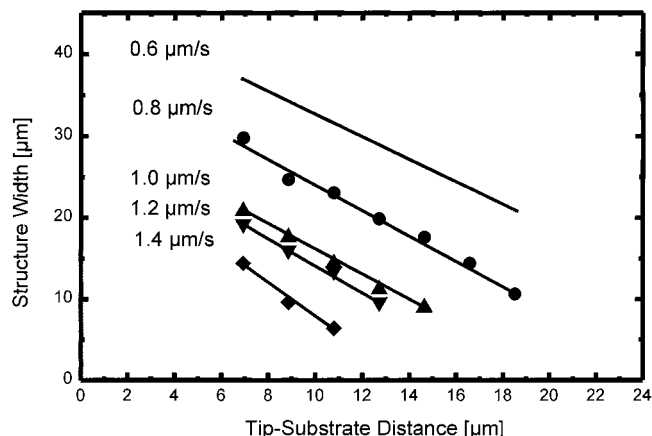


Figure 6. Dependence of the structure width on the tip-substrate distance at different scan rates. Data taken from Figure 5.

progress of the experiment. The MnO_2 layer has proven to be sufficiently thick to keep the oxidation of the monomers and oligomers running in all experiments.

As shown in Figure 8, the fabrication of microstructures of polythiophene using this new concept is flexible, highly reproducible, and repeatable. An analysis of the generated structures has been performed with the SECM to obtain information about the conductivity of the synthesized polymer. The reading process is based on the variation in the reduction current of the mediator ferricyanide $\text{K}_3[\text{Fe}(\text{CN})_6]$ as a function of the tip location. A comparison between an optical picture and a SECM image of the same area is shown in Figure 9. The analysis is very reproducible, and the structures can be clearly identified. This surface analysis shows the

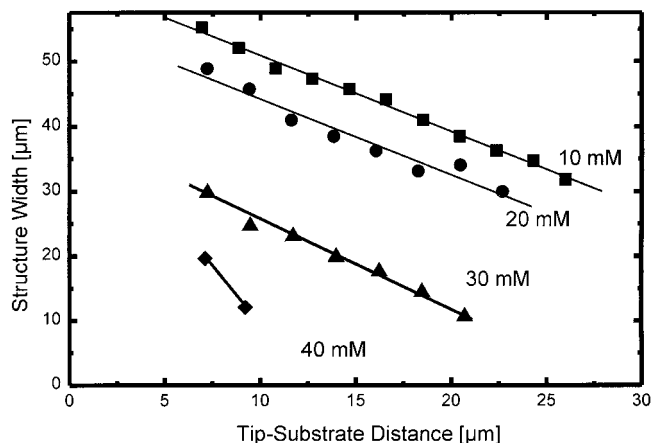


Figure 7. Dependence of the structure width on the tip-substrate distance at different scavenger concentrations for a scan rate of 0.8 $\mu\text{m}/\text{s}$ and conditions as given in Figure 5. The distance has been previously determined by feedback approach curves reducing ferricyanide.

difference in conductivity between the polymer and the manganese dioxide substrate. However, the absolute conductivity of polythiophene could not be established because of the higher background conductivity of the MnO_2 surface.

4. Conclusions

A novel method for the deposition of micropatterns of conducting polymers based on the scanning electrochemical microscope has been developed and found to be suitable for monomers with high solubilities in water. The galvanostatic oxidation of the mediator and the introduction of a chemical lens produced well-defined,

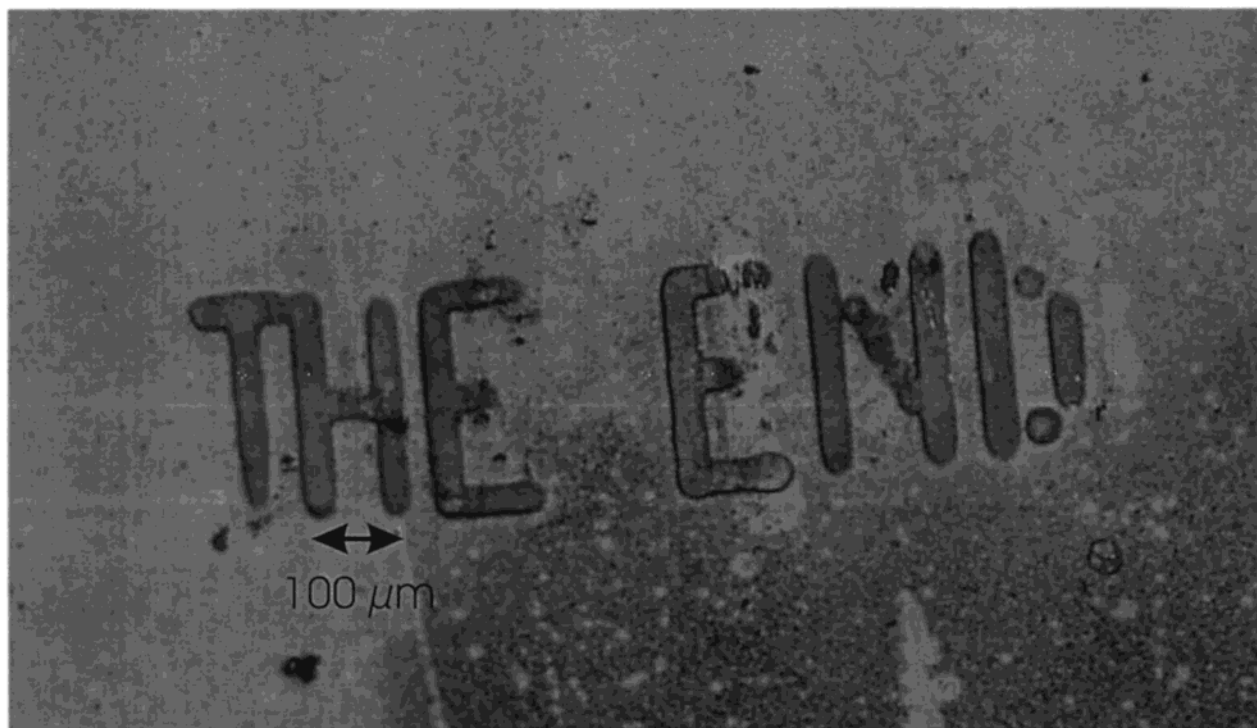


Figure 8. Tip = 10- μm Pt; RG = 10; electrolyte = 40 mM KNO_2 , 20 mM thiophene, 10 mM $\text{K}_3[\text{Fe}(\text{CN})_6]$, 10 mM NaHCO_3 . Galvanostatic process = 20 nA; scan rate = 0.8 $\mu\text{m}/\text{s}$ at a distance of 8 μm from the surface; pattern width = 20 μm .

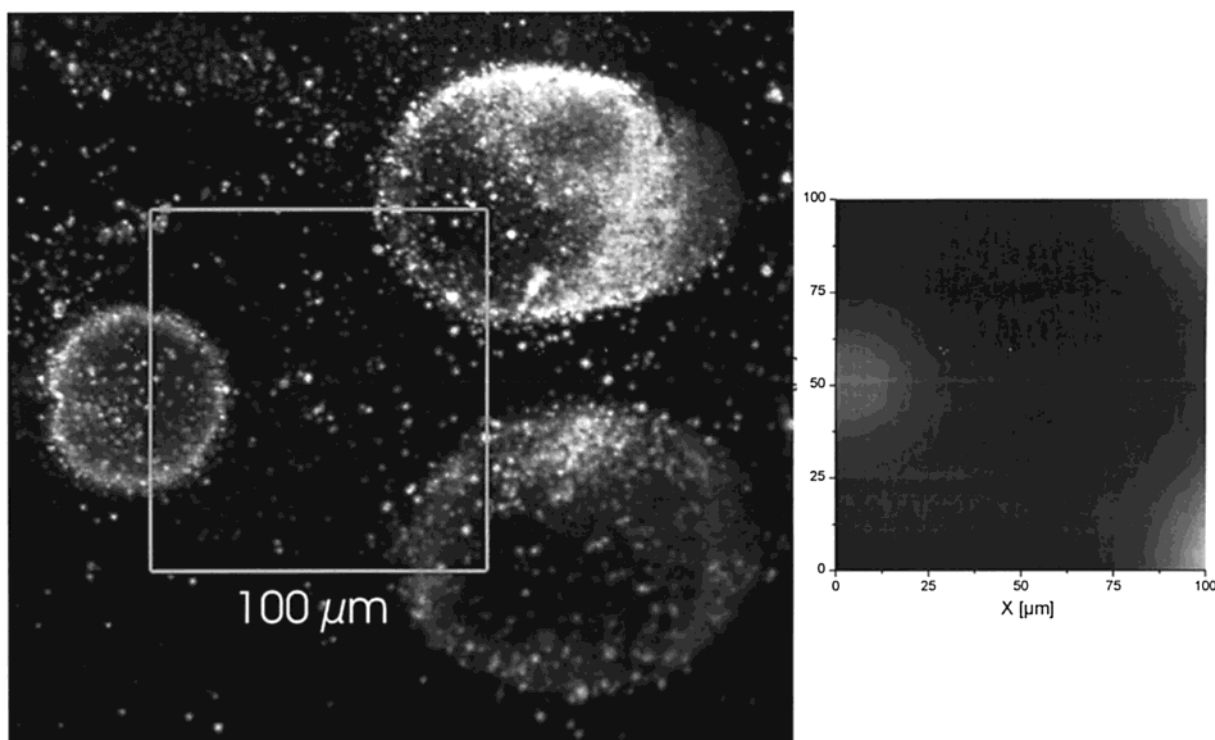


Figure 9. Comparison between an optical picture and a SECM image of the same area. Tip = 10- μm Pt; RG = 10; electrolyte = 40 mM KNO_2 , 20 mM thiophene, 10 mM $\text{K}_3[\text{Fe}(\text{CN})_6]$, 10 mM NaHCO_3 . For polymerization, $E = +1.2$ V for 150 s at 10 μm from the surface. For imaging, $E = -0.2$ V; scan rate = 10 $\mu\text{m}/\text{s}$ at a distance of 8 μm from the surface.

regular, and thin microstructures of polythiophene with a lateral resolution as small as 8–10 μm . The effects of scavenger concentration, tip–surface distance, and scan speed on the structure's width were investigated. Experiments led to the conclusion that the width of the patterns decreases as the scan rate, the tip–substrate distance, and the scavenger concentration increase. Moreover, a linear dependence between structure width

and tip–substrate distance was established. The results of the structural analysis are reproducible and illustrate the difference in conductivity between the manganese dioxide surface and the polymer.

Acknowledgment. We gratefully acknowledge the financial support of the BMBF and the DFG.

CM001062R